Electric control of exchange bias in multiferroic hexaferrite $Ba_{0.4}Sr_{1.6}Mg_2Fe_{12}O_{22}$

Kun Zhai,[1,2] Yisheng Chai,[3] Junzhuang Cong,[1] Dashan Shang,[1] and Young Sun[1,2,*]

[1]*Beijing National Laboratory for Condensed Matter Physics, Institute of Physics, Chinese Academy of Sciences, Beijing 100190, China*

[2]*School of Physical Sciences, University of Chinese Academy of Sciences, Beijing 100190, China*

[3]*School of Physics, Chongqing University, Chongqing 400044, China*

(Received 22 June 2018; revised manuscript received 31 August 2018; published 4 October 2018)

Electric field reversal of large magnetization has been achieved in the multiferroic hexaferrite $Ba_{0.4}Sr_{1.6}Mg_2Fe_{12}O_{22}$ with conical spin structures. The variation of magnetization depends on the sweeping rate of the applied electric field, leading to a significant fatigue effect. Such a slow dynamical behavior is attributed to the hysteresis magnetization process facilitated by the electric field. Moreover, the M-H hysteresis loop can be manipulated by external electric fields, causing either a positive or negative exchange bias phenomenon. The role of the electric field acting as a bias magnetic field on the magnetic hysteresis loop is discussed in terms of the pinning of magnetic domains by conjugated ferroelectric domains.

DOI: 10.1103/PhysRevB.98.144405

I. INTRODUCTION

Magnetoelectric (ME) multiferroics are promising candidates that could enable the mutual control of electric polarization (P) by magnetic field (H) and magnetization (M) by electric field (E) [1–8]. In particular, the control of M by E has attracted much attention in recent years for its intriguing fundamental physics and potential applications [9–11]. Although a large number of multiferroic materials have been discovered in the past decade, the modulating amplitude of M by E is usually small and the converse ME coefficient ($\alpha_E = \mu_0 dM/dE$) is quite low, which are major obstacles to applications.

To achieve large ME effects, the spin-driven ferroelectrics (type-II multiferroics) [12] are considered to be promising candidates. Their ferroelectricity is induced by noncollinear or collinear spin structures which break the space inversion symmetry. The microscopic origin of the spin-induced P is mainly due to an inverse Dzyaloshinskii–Moriya (DM) interaction [13], spin current theory (the KNB model) [14], or the exchange striction mechanism [15], respectively. The magnitude of P is usually two to three orders smaller than that of traditional ferroelectrics. However, a large ME coefficient ($\alpha_H = dP/dH$) can be found in some spin-driven ferroelectrics with noncollinear magnetic order due to the sensitive tuning of spin structure by low magnetic fields [7,16,17]. Additionally, E control of M can be realized in these materials via the accompanied large converse ME coefficient [7,16].

Among various multiferroic materials, multiferroic hexaferrites with tunable conical magnetic structure show prominent direct and converse ME effects [18–25]. For example, Chai *et al.* reported reversal of magnetization by E at 30 K in $Ba_{0.5}Sr_{1.5}Zn_2(Fe_{0.92}Al_{0.08})_{12}O_{22}$ [7]. Hirose *et al.* reported E control of M at room temperature in $BaSrCo_2Fe_{11}AlO_{22}$ [11]. Recently, giant direct and converse ME effects have been reported in $Ba_{0.4}Sr_{1.6}Mg_2Fe_{12}O_{22}$ [16]. The change of M induced by E exceeds $5.3\,\mu_B$/f.u. and the maximum converse ME coefficient is as high as 32 000 ps/m at 10 K, setting a record for single-phase multiferroics. However, the microscopic mechanism of the change of magnetization or magnetic structure with applied E field has not been well studied.

In this work, we have further studied in detail the converse ME effect in $Ba_{0.4}Sr_{1.6}Mg_2Fe_{12}O_{22}$ under both continuous and pulsed electric fields. In addition to the E reversal of M as reported in our previous work [16], we have found more interesting ME phenomena. The variation of M depends on the sweeping rate of the applied E, leading to a significant fatigue effect. The M-H hysteresis loop can be controlled by applying the E field, giving rise to either positive or negative exchange bias phenomenon. The role of applied E is to induce simultaneous rotation of P and M vectors inside the multiferroic domains in the ab plane. The E-biasing effect on the M-H loop is attributed to the conversion between electrostatic and Zeeman energies.

II. EXPERIMENTS

A $Ba_{0.4}Sr_{1.6}Mg_2Fe_{12}O_{22}$ single crystal was synthesized from Na_2O-Fe_2O_3 flux in air [26]. The starting chemicals were mixed with a molar ratio 3.938% $BaCO_3$, 15.752% $SrCO_3$, 19.69% MgO, 53.61% Fe_2O_3, and 7.01% Na_2O and melted in a Pt crucible at 1420 °C for 20 h, followed by a thermal recycle. The crystals were slowly precipitated from high temperature flux when cooled to 1100 °C at the rate of 1 °C/h. The H-dependent dielectric constant and ME current were performed in a cryogen-free superconducting magnet system (Oxford Instrument, Teslatron PT) using a LCR meter (Aglient, 4980A) and an electrometer (Keithley 6517B), respectively. The M under E field was measured in a magnetic property measuring system (MPMS, Quantum Design) using a modified sample holder. Before the ME current

*Author to whom correspondence should be addressed: youngsun@iphy.ac.cn

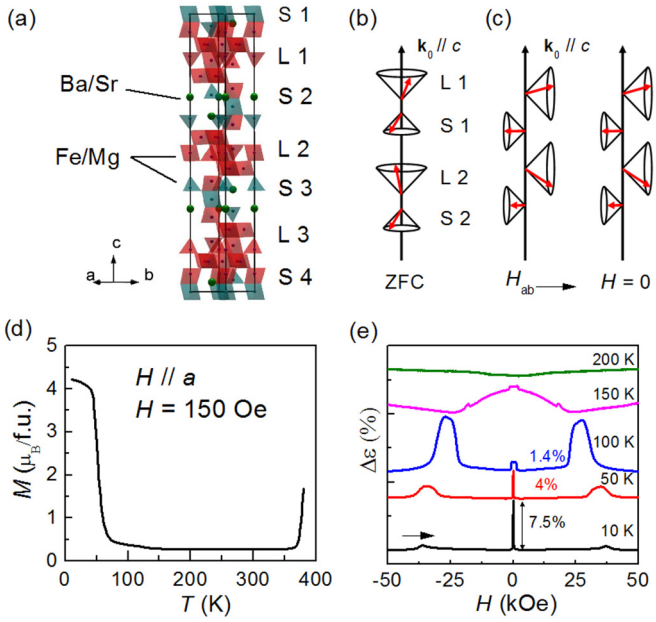

FIG. 1. (a) Crystal structure of $Ba_{0.4}Sr_{1.6}Mg_2Fe_{12}O_{22}$. L and S denote small and large magnetic blocks, respectively. (b) The magnetic structure of longitudinal cone and (c) transverse cone. (d) Temperature dependence of magnetization with $H = 150$ Oe along the a axis. Before the measurements, the sample is cooled to 2 K and the magnetic field is set to 50 kOe, then ramped to 150 Oe, followed by an increase in temperature with the rate of 2 K/s. (e) The relative change of dielectric constant $\Delta\varepsilon$ dependence of H at different temperatures. The change of dielectric peaks is obtained by $\Delta\varepsilon(H_{\max}) = [\varepsilon(H_{\max}) - \varepsilon(50\,\text{kOe})]/\varepsilon(50\,\text{kOe})$.

measurements at 10 K, ME poling procedures were applied as follows: H was first set to 50 kOe along the [100] direction and an E of 750 kV/m was applied along the [120] direction of the crystal. Then H was ramped to 5 kOe. After that, the E was removed and the electrodes were short-circuited for 30 min. The ME current was measured by sweeping the magnetic field at the rate of 20 Oe/s. For the magnetization under electric field measurements, a similar ME poling sequence with the poling field of 2.5 MV/m was applied and the final magnetic field was set to 0 Oe.

III. RESULTS AND DISCUSSION

Figure 1(a) shows the crystal structure of $Ba_{0.4}Sr_{1.6}Mg_2Fe_{12}O_{22}$. Its space group is $R\bar{3}m$, which cannot generate a spontaneous polarization. Two repeating magnetic units, which are characterized by large (L) magnetic block and small (S) magnetic block, respectively, stack along hexagonal c axis. In each block, magnetic moments on Fe site are collinearly arranged, while Mg^{2+} ions randomly distribute at the tetrahedral and octahedral sites [27]. The Fe-O-Fe superexchange interaction across the boundary of L and S blocks can be affected by Ba/Sr sites, which is vital for producing a noncollinear structure [28]. At low temperatures (T), the magnetic structure becomes an incommensurate longitudinal cone (LC) [Fig. 1(b)]. With in-plane H_{ab}, the magnetic structure becomes an commensurate transverse cone (TC) [Fig. 1(c)]. However, when the magnetic field is swept back to zero, the metastable TC magnetic structure was maintained rather than recovering to the LC phase. The TC structure can lead to an electric polarization perpendicular to both the H and [001] directions due to the spin current model $P \propto \sum_{ij} \mathbf{e}_{LS} \times (\mathbf{S}_L \times \mathbf{S}_S)$, where adjacent block $\mathbf{S}_S$ and $\mathbf{S}_L$ is connected by a unit vector $\mathbf{e}_{LS} \| [001]$. Here, the polarization in $Ba_{0.4}Sr_{1.6}Mg_2Fe_{12}O_{22}$ is assumed to be generated between the L and S blocks instead of single magnetic ions inside them.

Figure 1(d) shows the temperature dependence of magnetization along the [100] direction. To measure the M-T curve, we first applied an external $H = 50$ kOe along the [100] direction at 10 K to reach a ferrimagnetic phase at high magnetic fields, then set H down to 150 Oe to obtain a TC phase at low magnetic fields [29]. With increasing temperature, a steep decrease of magnetization happens around 50 K, indicating the induced TC phase gradually becomes the LC phase at higher T. The M-T curve becomes flat above 80 K, indicating a proper screw magnetic structure. Above 380 K, M sharply increases, implying a collinear ferrimagnetic phase stabilizes at higher temperatures.

Figure 1(e) shows the relative change of dielectric constant $\Delta\varepsilon = [\varepsilon(H) - \varepsilon(50\,\text{kOe})]/\varepsilon\,(50\,\text{kOe})$ ($E \| [20]$) with sweeping $H(\| [100])$ from -50 to 50 kOe at different temperatures. In the high H region, the clear broad peaks can be observed at all selected temperatures, representing the boundaries between the high H paraelectric (PE) and the low H ferroelectric (FE) phase. In the low H region, a single dielectric peak around zero field gives the over 7% change of ε at 10 and 50 K. The large $\Delta\varepsilon$, which indicates the direct reversal of FE/TC domains in the ab plane, can be observed up to 50 K, which coincides with the temperature region of stabilizing the TC magnetic structure around zero H [30]. The FE domain and magnetic in-plane domains are clamped with each other and four domain states $(+M, +P)$, $(-M, +P)$, $(-M, -P)$, $(+M, -P)$ could coexist [2]. The reversal of magnetization is accompanied with the reversal of polarization and thus a large ME coupling effect associated with the change of magnetic structure is expected. At higher T, the dielectric peak around zero field broadens for 100 and 150 K, implying a change of magnetic structure. Above 150 K, a leaky feature can be observed on the $\Delta\varepsilon(H)$ curve.

We further measured the P-H curve in the FE/TC region at 10 K [Fig. 2(a)]. The P-H hysteresis loops confirm a direct reversal of the FE domain around zero H, as shown in Fig. 2(a). The saturated polarization is 245 μC/m^2 and the coercive magnetic field is 100 Oe. The drastic reversal of polarization around the coercive field produces a large direct ME coefficient. The maximum ME coefficient $\alpha_H = \mathrm{d}P/\mathrm{d}H$ was estimated to be 33 000 ps/m [16], which is the highest value in single-phase multiferroics as far as we know. The reversal of polarization is repeatable in the low magnetic field range, as shown in Fig. 2(b). The polarization shows a periodical change as the function of time when the magnetic field oscillates in the range between -2.5 and 2.5 kOe. We noticed that the coercive field of this sample is much larger than that in $Ba_{0.5}Sr_{1.5}Zn_2(Fe_{0.92}Al_{0.08})_{12}O_{22}$ with a smaller α_H [2]. It usually indicates a larger in-plane magnetic anisotropy for $Ba_{0.4}Sr_{1.6}Mg_2Fe_{12}O_{22}$.

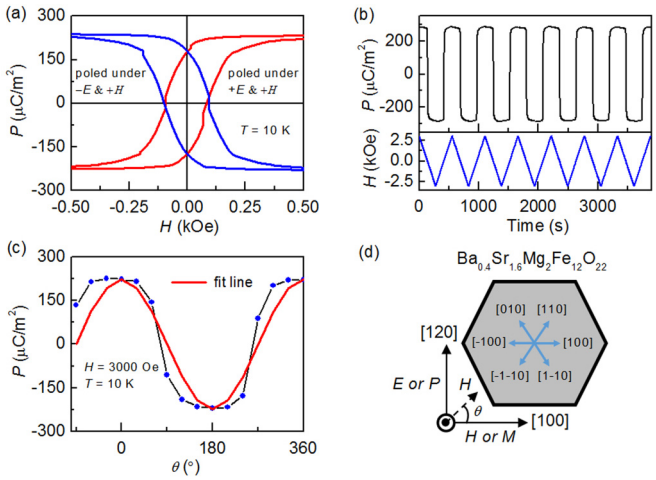

FIG. 2. (a) The P-H loops after $-E$ & $+H$ and $+E$ & $+H$ poling procedures. (b) Cyclic reversal of P with H in the range of 2.5 kOe and −2.5 kOe at 10 K. (c) P measured under different θ values. (d) The configuration of measurement. The H applied or M measured is along the [100] direction and the E applied or P measured is along the [120] direction. The dashed line represents the direction of H and θ denotes the angle between H and the [100] axis when the sample is rotated in the ab plane. Magnetic moments prefer to align along the blue arrows that denote the crystal orientation.

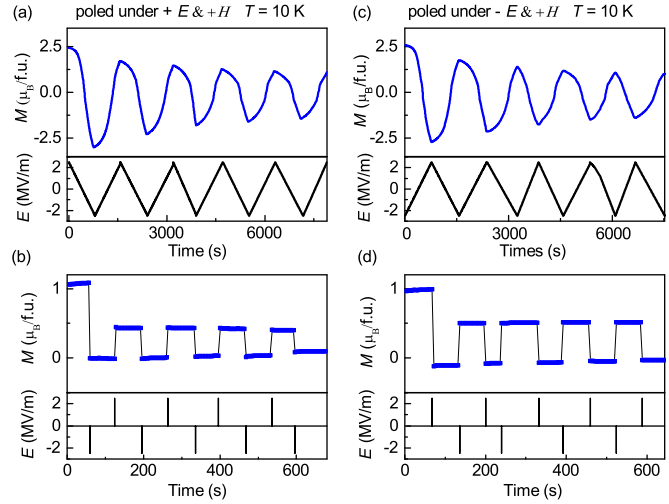

FIG. 3. Periodic modulations of M under continually changed electric field after (a) $+E$, $+H$ and (c) $-E$, $+H$ poling procedures. Magnetization change with plus E after (b) $+E$, $+H$ and (d) $-E$, $+H$ poling conditions. The positive E is 2.5 MV/m and the negative E is −2.5 MV/m. The repeating change of magnetization under the square wave of electric field with a duration of 1 s for two poling procedures

The TC phase has a magnetic easy-plane with a sixfold hexagonal in-plane anisotropy, as shown in Fig. 2(d). In the magnetization reversal process, the magnetization vector in a single magnetic domain will be pinned to one of the six directions until H is large enough, producing a clear hysteresis in the M-H loop, or the P-H loop in our case since P and M always rotate together to keep a perpendicular relationship in a single domain. To check this, we measured the in-plane angle (θ) dependent polarization along [120], where θ represents the angle between in-plane H and the [100] direction of the crystal, as shown in Fig. 2(d). We first applied the ME poling procedure at $\theta = 0^\circ$ then rotated H in the hexagonal plane and collected the ME current. Figure 2(c) displays the measured polarization at $H = 3$ kOe as a function of θ. The P-θ curve clearly shows a deviation from the ideal cosine wave behavior, indicating a relatively larger in-plane magnetic anisotropy due to the pinning of M and P vector under small H.

The large in-plane anisotropy may affect the converse ME effect of $Ba_{0.4}Sr_{1.6}Mg_2Fe_{12}O_{22}$. We investigated the repetition of the E modulation of M. The ME poling procedures ($+E$, $+H$ or $-E$, $+H$) were carried out to obtain a single domain state. The E was further swept between +2.5 MV/m and −2.5 MV/m for several times to measure the M change under E circles. The M changes with E in the same trend with $+E$ and $+H$ poling [Fig. 3(a)], while in the opposite trend after $-E$, $+H$ poling history [Fig. 3(c)]. With oscillating E, the M changes in the range between 2.5 μ_B/f.u. and −2.8 μ_B/f.u. for both poling procedures, but gradually decays circle by circle. In contrast, the similar M change under E oscillation measurement in $Ba_{0.5}Sr_{1.5}Zn_2(Fe_{0.92}Al_{0.08})_{12}O_{22}$ only shows negligible decay behavior [2]. Therefore, the significant decay of M under repeated E sweeping is likely to be attributed to the stronger in-plane anisotropy and a larger coercive field in the M-E curve of $Ba_{0.4}Sr_{1.6}Mg_2Fe_{12}O_{22}$. The larger the magnetic anisotropy is, the stronger the application of E is required to induce the simultaneous rotation of the P and M vectors inside the clamped domains in the ab plane.

The decay of magnetization can also be seen under repeated E pulses with a duration time of 1 s, as shown in Figs. 3(b) and 3(d). Figure 3(b) presents the change of M under E pulses after $+E$, $+H$ poling. A negative E pulse of −2.5 MV/m can change the initial M of 1.05 μ_B/f.u. and preserve the value without E. A subsequent positive pulse 2.5 MV/m results in a jump of M to 0.5 μ_B/f.u., lower than the initial value. For the subsequent train of electric field pulses, the switching of M still shows a slow fatigue behavior. The M change under E pulses after the $-E$ and $+H$ poling procedure shows very similar decaying behavior, as shown in Fig. 3(d).

We further studied the change of M under different E field sweeping rates. In Fig. 4(d), M can only approach −1.4 μ_B/f.u. with a sweeping time of 880 s from $E =$ +2.5 MV/m to −2.5 MV/m. In contrast, M can reach −2.3 μ_B/f.u. with the total E sweeping time of 4400 s, which is two times longer in terms of M change than that of the fast sweep process. It shows that to overcome the high magnetic anisotropy, a longer duration time under E is necessary for nucleation and propagation of FE/TC clamped domain walls.

From the above experimental results, the E seems to play a role as H does in manipulating the change or reversal of M and the observed fatigue effect is very similar to the "minor loop" effect in terms of the magnetic hysteresis loop. To investigate the effect of the electric field on the TC phase in $Ba_{0.4}Sr_{1.6}Mg_2Fe_{12}O_{22}$, we performed the low field M-H loop under different E bias, as shown in Fig. 5(a). The M-H hysteresis loops are shifted nearly without any distortion along the H-axis direction upon the application of E, where

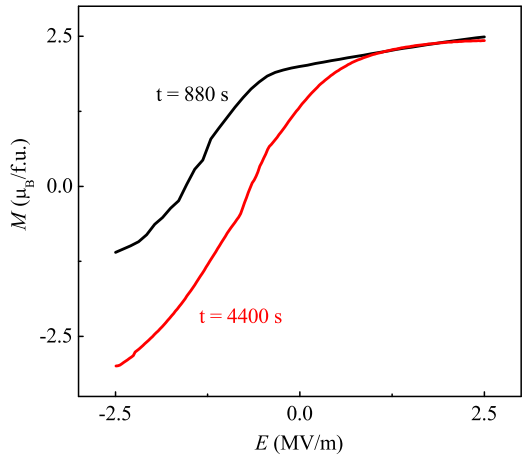

FIG. 4. The initial change of magnetization after positive $+E$ and $+H$ poling with H scanning from 2.5 MV/m to -2.5 MV/m at different rates.

the direction depends on the polarity of E. The maximum shift H_{EB} reaches -30 Oe and $+35$ Oe for $E = \pm 1.7$ MV/m, respectively, which is like a typical exchange-bias effect.

Exchange-bias phenomena is generally assigned to the exchange coupling at different magnetic interfaces that causes a pinning of magnetization. The exchange bias induced by E field can be explained as follows. The application of E modifies the ground state energy of $\pm M$ due to the electrostatic energy, $\pm PE$. The Landau free energy of ferromagnetism considering a conjugate field H_{EB} induced by P can be written as

$$\Phi(P, T, M) = \Phi_0 + a(T\text{-}T_c)M^2 + bM^4 + MH_{EB} \ldots, \quad (1)$$

where M is the order parameter and H_{EB} is the exchange-bias field from E. As explained in Fig. 5(c), the asymmetrically distorted double well potential without the application of external H will be totally compensated by the presence of H_{EB} that satisfies $-MH_{EB} = PE$. Therefore, the M-H loop should be shifted along the H axis by $H_{EB} = -\frac{PE}{M}$. Thus, the amount of the shift is proportional to E, and its sign depends on the polarity of E.

To test the above theoretical analysis, the experimentally obtained values of $|PE|$ and $|MH_{EB}|$ from the E-biased M-H data are compared in Fig. 5(b). The values of spontaneous M and P of TC phase are selected at $H = 500$ Oe. The diagonal line in Fig. 5(b) represents the $|PE| = |MH_{EB}|$ relationship and the calculated data points largely fall close to this line with small deviations due to measurement uncertainties. Therefore, the $-MH_{EB} = P\Delta E$ relation is reliably confirmed in the experiments, validating the proposed interpretation of

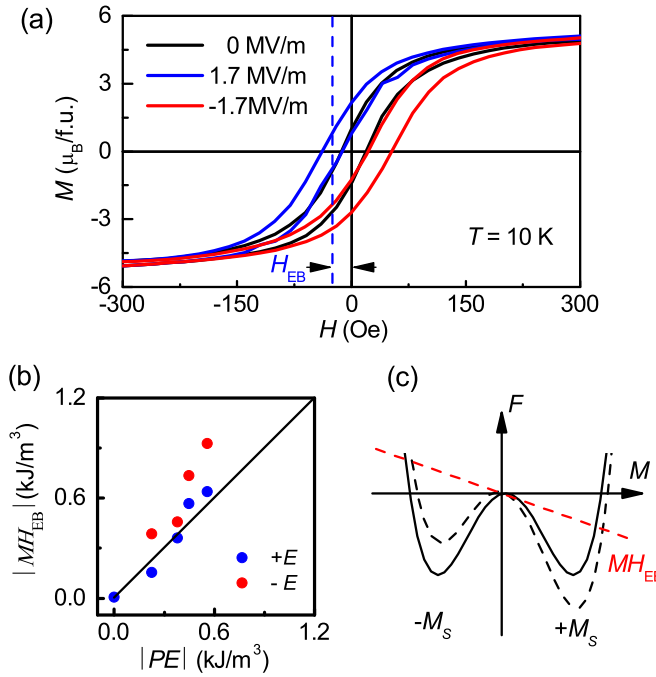

FIG. 5. (a) The M-H loops measured under -1.7, 0, and 1.7 MV/m electric fields. (b) The bias of magnetic field at different electric field. (c) Free energy with double minimum show asymmetric deformation with E applied.

exchange bias effect from the electrostatic energy. It is worth mentioning that the reversed effect of magnetic biasing of a ferroelectric hysteresis loop has been observed in a multiferroic orthoferrite $Dy_{0.7}Tb_{0.3}FeO_3$ [31].

IV. CONCLUSION

The noncollinear magnetic structure between magnetic blocks rather than single magnetic ions is in favor of producing large ME effects, as we demonstrated in the multiferroic hexaferrite $Ba_{0.4}Sr_{1.6}Mg_2Fe_{12}O_{22}$. The time-dependent change of magnetization with continuous or pulse E field suggests that role of E field is to drive nucleation and propagation of magnetic domains. The low field M-H loop under a different E field shows exchange-bias behavior, which implies that an effective inner H field is induced by E. This is ascribed to the pinning effect between the conjugated ferroelectric and magnetic domains in magnetic-order-induced multiferroics.

ACKNOWLEDGMENTS

This work was supported by the National Natural Science Foundation of China (Grant No. 11534015, 51725104, 11674384) and the National Key Research and Development Program of China (Grant No. 2016YFA0300701). Y.S. also acknowledges the support from the Strategic Priority Research Program of the Chinese Academy of Sciences (Grants No. XDB07030200).

[1] T. Kimura, T. Goto, H. Shintani, K. Ishizaka, T. Arima, and Y. Tokura, Nature (London) **426**, 55 (2003).

[2] W. Eerenstein, N. D. Mathur, and J. F. Scott, Nature (London) **442**, 759 (2006).

[3] M. Fiebig, T. Thomas, D. Meier, and M. Trassin, Nat. Mater. Rev. **1**, 16046 (2016).
[4] F S.-W. Cheong and M. Mostovoy, Nat. Mater. **6**, 21 (2007).
[5] S. Dong, J.-M. Liu, S.-W. Cheong, and Z. Ren, Adv. Phys. **64**, 519 (2015).
[6] Matsukura, Y. Tokura, and H. Ohno, Nat. Nanotech. **10**, 209 (2015).
[7] Y. S. Chai, S. Kwon, S. H. Chun, I. Kim, B.-G. Jeon, K. H. Kim, and S. Lee, Nat. Commun. **5**, 4208 (2014).
[8] J. Shen, D. Shang, Y. Chai, Y. Wang, J. Cong, S. Shen, L. Yan, W. Wang, and Y. Sun, Phys. Rev. Appl. **6**, 064028 (2016).
[9] K. Zhai, D. Shang, Y. Chai, G. Li, J. Cai, B. Shen, and Y. Sun, Adv. Funct. Mater. **28**, 1705771 (2018).
[10] N. Lu, P. Zhang, Q. Zhang, R. Qiao, Q. He, H. B. Li, Y. Wang, J. Guo, D. Zhang, Z. Duan, Z. Li, M. Wang, S. Yang, M. Yan, E. Arenholz, S. Zhou, W. Yang, L. Gu, C. W. Nan, J. Wu, Y. Tokura, and P. Yu, Nature **546**, 124 (2017).
[11] S. Hirose, K. Haruki, A. Ando, and T. Kimura, Appl. Phys. Lett. **104**, 022907 (2014).
[12] D. Khomskii, Physics **2**, 20 (2009).
[13] I. A. Sergienko and E. Dagaotto, Phys. Rev. B **73**, 094434 (2006).
[14] H. Katsura, N. Nagaosa, and A. V. Balatsky, Phys. Rev. Lett. **95**, 057205 (2005).
[15] Y. J. Choi, H. T. Yi, S. Lee, Q. Huang, V. Kiryukhin, and S.-W. Cheong, Phys. Rev. Lett. **100**, 047601 (2008).
[16] K. Zhai, Y. Wu, S. P. Shen, W. Tian, H. B. Cao, Y. S. Chai, B. C. Chakoumakos, D. S. Shang, L. Q. Yan, F. W. Wang, and Y. Sun, Nat. Commun. **8**, 519 (2017).
[17] Y. Tokunaga, Y. Taguchi, T. Arima, and Y. Tokura, Nat. Phys. **8**, 838 (2012).
[18] S. H. Chun, Y. S. Chai, B.-G. Jeon, H. J. Kim, Y. S. Oh, I. Kim, H. Kim, B. J. Jeon, S. Y. Haam, J.-Y. Park, S. H. Lee, J.-H. Chung, J.-H. Park, and K. H. Kim, Phys. Rev. Lett. **108**, 177201 (2012).
[19] S.-P. Shen, X.-Z. Liu, Y.-S. Chai, A. Studer, K. Rule, K. Zhai, L.-Q. Yan, D.-S. Shang, F. Klose, Y.-T. Liu, D.-F. Chen, and Y. Sun, Phys. Rev. B **95**, 094405 (2017).
[20] K. Okumura, T. Ishikura, M. Soda, T. Asaka, H. Nakamura, Y. Wakabayashi, and T. Kimura, Appl. Phys. Lett. **98**, 212504 (2011).
[21] T. Kimura, G. Lawes, and A. P. Ramirez, Phys. Rev. Lett. **94**, 137201 (2005).
[22] S. Ishiwata, Y. Taguchi, H. Murakawa, Y. Onose, and Y. Tokura, Science **319**, 1643 (2008).
[23] Y. Tokunaga, Y. Kaneko, D. Okuyama, S. Ishiwata, T. Arima, S. Wakimoto, K. Kakurai, Y. Taguchi, and Y. Tokura, Phys. Rev. Lett. **105**, 257201 (2010).
[24] Y. Kitagawa, Y. Hiraoka, T. Honda, T. Isgukura, H. Nakamura, and T. Kimura, Nat. Mater. **9**, 797 (2010).
[25] F. Wang, T. Zou, L.Q. Yan, Y. Liu, and Y. Sun, Appl. Phys. Lett. **100**, 122901 (2012).
[26] N. Momozawa, M. Mita, and H. Takei, J. Cryst. Growth **83**, 403 (1987).
[27] N. Momozawa, Y. Nagao, S. Utsumi, M. Abe, and Y. Yamaguchi, J. Phys. Soc. Jpn. **70**, 2724 (2001).
[28] N. Momozawa, Y. Yamaguchi, and M. Mita, J. Phys. Soc. Jpn. **55**, 1350 (1986).
[29] S. P. Shen, Y. S. Chai, and Y. Sun, Sci. Rep. **5**, 8254 (2014).
[30] S. P. Shen, L. Q. Yan, Y. S. Chai, J. Z. Cong, and Y. Sun, Appl. Phys. Lett. **104**, 032905 (2014).
[31] Y. Tokunaga, Y. Taguchi, T. Arima, and Y. Tokura, Phys. Rev. Lett. **112**, 037203 (2014).